

## Chapter 2

# Physical Measurements

It is absolutely infeasible to do localization without knowledge of the physical world. According to the capabilities of diverse hardware, we classify the measuring techniques into six categories (from fine grained to coarse grained): location, distance, angle, area, hop count, and neighborhood, as shown in Fig. 2.1.

Among them, the most powerful physical measurement is directly obtaining the position without any further computation. GPS is such a kind of infrastructure. Besides, the other five measurements are used in the scenarios of positioning an unknown node by giving some reference nodes. Distance and angle measurements are obtained by ranging techniques, while hop count and neighborhood are basically based on radio connectivity. In addition, area measurement relies on either ranging or connectivity depending on how the area constrains are formed.

### 2.1 Distance Measurements

Many physical quantities are distance related, such as the received radio signal strength, the propagation time of an acoustic signal. Investigating the physical characteristics of signals, researchers form the basic quantity-distance models that convert the measured signals to the physical distances. In this section, we mainly focus on the typical ranging techniques: radio signal strength (RSS), time of arrival (ToA), and time difference of arrival (TDoA).

#### 2.1.1 Radio Signal Strength

RSS-based ranging techniques rely on the fact that the strength of radio signal diminishes during propagation. As a result, the understanding of radio attenuation helps to map signal strength to distance.

A common assumption is that the propagation distances  $d$  is much larger than the square of the antenna size divided by the wavelength. In an idealized free space, RSS is proved to be linear with the inverse square of the distance  $d$  between the

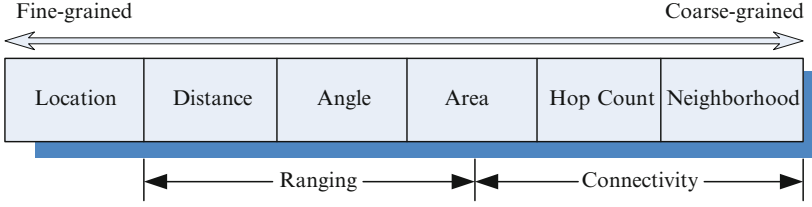


**Fig. 2.1** Physical measurements

transmitter and the receiver. Let  $P_r(d)$  denote the received power at distance  $d$ . The value of  $P_r(d)$  follows the Friis equation [27]:

$$P_r(d) = \left( \frac{\lambda}{4\pi d} \right)^2 P_t G_t G_r,$$

where  $P_t$  is the transmitted power,  $G_t$  and  $G_r$  are the antenna gain of the transmitting and receiving antennas, respectively, and  $\lambda$  is the wavelength of the transmitter signal in meters.

In practice, several factors, such as shadowing and reflection, may affect the radio signal propagation as well as the received power. Unfortunately, these factors are environment dependent and unpredictable. As the shadowing effects cannot be precisely tracked, they are usually modeled as a log-normally distributed random variable. Considering the randomness, signal strength diminishes with distance according to a power law. One model used for wireless radios is as follows [28]:

$$P_r(d) = P_0(d_0) - \eta 10 \log_{10} \left( \frac{d}{d_0} \right) + X_\sigma,$$

where  $P_r(d)$  denotes the received power at distance  $d$  and  $P_0(d_0)$  denotes the received power at some reference distance  $d_0$ ,  $\eta$  denotes the path-loss exponent, and  $X_\sigma$  denotes a log-normal random variable with variance  $\sigma^2$  that accounts for fading effects. If the path-loss exponent for a given environment is known, the received signal strength can be used to estimate the distance. By this model, the maximum likelihood estimate of distance  $d$  is as follows [27]:

$$\hat{d} = d_0 \left( \frac{P_r}{P_0(d_0)} \right)^{-1/\eta}.$$

In addition, the relationship between the estimated distance and the ground-truth distance is

$$\hat{d} = d 10^{-\frac{X_\sigma}{10\eta}} = d e^{-\frac{2X_\sigma}{\eta}},$$

where  $\alpha = \ln 10/10$ . Hence, the expected value of the estimated distance is

$$E(\hat{d}) = \frac{1}{\sqrt{2\pi}\sigma} \int_{-\infty}^{\infty} d e^{-\alpha X_{\sigma}/\eta} e^{-X_{\sigma}^2/2\sigma^2} dX_{\sigma} = d e^{(\alpha^2/2)(\sigma^2/\eta^2)}.$$

Thus the maximum likelihood estimate is biased from the ground-truth distance. Hence, an unbiased estimate is given by

$$\hat{d} = d_0 \left( \frac{P_r}{P_0(d_0)} \right)^{-1/\eta} e^{-(\alpha^2/2)(\sigma^2/\eta^2)}.$$

The ranging noise occurs because radio propagation tends to be highly dynamic in complicated environments. Although RSS-based ranging contains noises on the order of several meters (or even worse performance) [29], it is widely used in many real-world systems because RSS is a relatively “cheap” solution without any special hardware, as all nodes are supposed to have radios. It is believed that more careful physical analysis of radio propagation may allow better use of RSS data. Nevertheless, the breakthrough technology is not there today.

### 2.1.2 Time of Arrival (ToA)

For a signal with known velocity (e.g., acoustic signal), measuring the propagation-induced time can straightforwardly indicate the transmitter–receiver separation distance. The key issue of this mechanism is to accurately measure the time of arrival (ToA). There are two categories of ToA-based distance measurement: the one-way propagation time estimation and the round-trip propagation time estimation.

#### 1) One-way propagation time estimation

Propagation delay, which can be calculated as  $t_i - t_0$ , is the time lag between the departure of a signal from a transmitter and the arrival at a receiver; in other words, it is the amount of time required for a signal to travel from a transmitter to a receiver. Assuming the speed of a signal  $v$ , the transmitter–receiver distance can be calculated by  $d = v(t_i - t_0)$ .

In the basic scheme of ToA, the receiver needs to know the time when the signal is sent from the transmitter. One method to release the requirement of time synchronization is the combined use of signals with different speeds, such as the ultrasound/acoustic and radio signals [30–32].

In such a scheme, each node is equipped with a speaker and a microphone, as illustrated in Fig. 2.2. Some systems use ultrasound while others use audible frequencies. The general ranging technique, however, is independent of any particular hardware.

The idea of ToA ranging is conceptually simple, as illustrated in Fig. 2.3. The transmitter first emits a radio signal. It waits some fixed internal of time,  $t_{\text{delay}}$

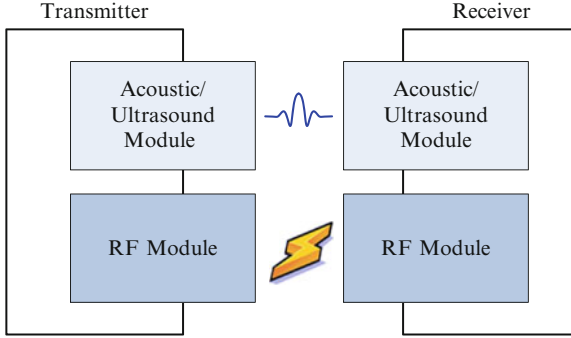


**Fig. 2.2** To A hardware model

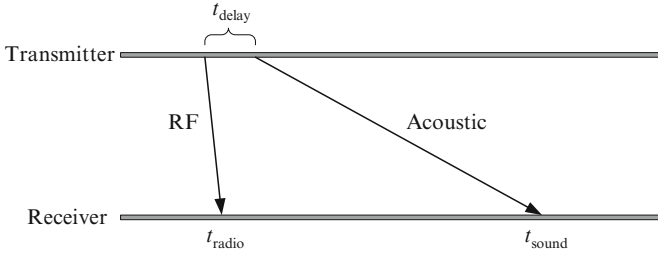


**Fig. 2.3** ToA computation model

(which might be zero), and then produces a fixed pattern of “chirps” on its speaker. When the receivers hear the radio signal, they record the current time,  $t_{\text{radio}}$ , and turn on their microphones. When their microphones detect the chirp pattern, they again record the current time,  $t_{\text{sound}}$ . Once they have  $t_{\text{radio}}$ ,  $t_{\text{sound}}$ , and  $t_{\text{delay}}$ , the receivers can compute the transmitter–receiver distance  $d$  by

$$d = \frac{v_{\text{radio}} v_{\text{sound}}}{v_{\text{radio}} - v_{\text{sound}}} (t_{\text{sound}} - t_{\text{radio}} - t_{\text{delay}}),$$

where  $v_{\text{radio}}$  and  $v_{\text{sound}}$  denote the speed of radio and sound waves, respectively. Since radio waves travel substantially faster than sound in air, the distance is then estimated as  $d = v_{\text{sound}} (t_{\text{sound}} - t_{\text{radio}} - t_{\text{delay}})$ . If radio and acoustic signals are designed to be transmitted simultaneously (i.e.,  $t_{\text{delay}} = 0$ ), the estimation can be further simplified as  $v_{\text{sound}} (t_{\text{radio}} - t_{\text{sound}})$ .

To A methods are impressively accurate under line-of-sight conditions. For instance, it is claimed in [31] that distance can be estimated with error no more than a few centimeters for node separations under 3 m. The cricket ultrasound system [30] can obtain centimeter accuracy over about 10-m range in indoor environments.

## 2) Round-trip propagation time estimation

One-way propagation time estimation requires synchronization between the nodes, because the computation relies on the timestamps recorded in both the nodes. One way to avoid synchronization is to use round trip time (RTT). In RTT measurement, nodes only need to report local time duration instead of the timestamps. The RTT estimate between two nodes, labeled as  $A$  and  $B$ , is as follows. Node  $A$  transmits a packet to node  $B$ . After receiving this packet, node  $B$  delays  $t_{\text{delay}}$ , and then replies node  $A$  by sending an acknowledgment packet. The RTT at  $A$  is determined by  $t_{RT} = 2t_{\text{flight}} + t_{\text{delay}}$ , where  $t_{\text{flight}}$  denotes the distance-induced propagation time of the signal. When node  $B$  reports the measured delay  $t_{\text{delay}}$ , node  $A$  can compute the time of signal propagation by  $t_{\text{flight}} = (t_{RT} - t_{\text{delay}})/2$ . However, RTT measurement suffers from the clock drift between the nodes, especially when  $t_{\text{flight}}$  is of the same level of the resolution of  $t_{RT}$  and  $t_{\text{delay}}$  measurements.

### 2.1.2.1 Symmetric Double Sided Two-Way Ranging (SDS-TWR)

When we adopt radio signal for the ToA-based distance measurement, the ranging mainly relies on the resolution of time measurement. There are two main sources of errors: the multipath effect and the time synchronization. Nanotron technologies proposes SDS-TWR to address such issues [33].

SDS-TWR adopts chirp spread spectrum (CSS) to provide fine resolution of a few nanoseconds for signal detection in spite of the multipath propagation and noises. CSS is a customized application of multidimensional multiple access (MDMA) for the requirements of battery-powered applications, where the reliability of the transmission and low power consumption are of special importance. CSS operates in the 2.45 GHz ISM band and achieves a maximum data rate of 2 Mbps. Each symbol is transmitted with a chirp pulse that has a bandwidth of 80 MHz and a fixed duration of 1  $\mu\text{s}$ .

To avoid time synchronization, the elapsed time is measured by round trip time (RTT). RTT is the time duration between the timestamp of sending a ranging signal and that of the acknowledgement. RTT uses highly predictable hardware-generated acknowledgement packets where MAC processing time assumed to be equal on both nodes. Note that the timestamps are processed on the physical layer, not on the application layer. Figure 2.4 illustrates the measurement procedure, where we show

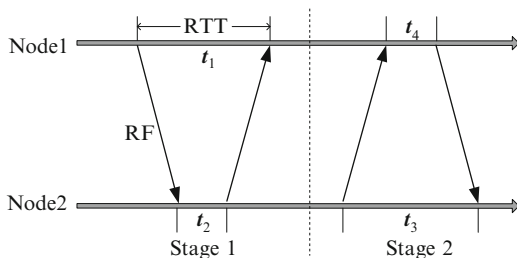


**Fig. 2.4** Symmetric double sided two-way ranging

the packet transfer according to the time lines of two nodes. There are two stages for SDS-TWR, each of which is a RTT measurement.

In stage 1, time measurement of node 2 begins only when it receives a packet from node 1 and then stops when it sends a packet back to node 1. Thus, the distance between node 1 and node 2 is given by

$$d = v(t_1 - t_2)/2,$$

where  $v$  denotes the speed of radio signal. Nevertheless, such a scheme suffers clock drift between the two nodes, because off-the-shelf oscillators can only provide timing resolution of several nanoseconds. To mitigate the clock drift, SDS-TWR conducts the ranging measurement twice and symmetrically. As shown in Fig. 2.4, the first ranging measurement is calculated based on a round trip from node 1 to node 2 and back to node 1. The second measurement is calculated based on a round trip from node 2 to node 1 and back to node 2. This double-sided ranging measurement zeroes out the errors of the first order due to the clock drift. Hence, the distance estimate is given by

$$d = v[(t_1 - t_2) + (t_3 - t_4)]/4.$$

### 2.1.2.2 BeepBeep

Recently, researchers [34] observe that two intrinsic uncertainties in ToA can contribute to ranging inaccuracy: the possible misalignment between the sender timestamp and the actual signal emission, and the possible delay of a sound signal arrival being recognized at the receiver. To eliminate such uncertainties, round-trip measurement techniques are introduced.

In general, many factors can cause uncertainties in a real system, such as the lack of real-time control, software delay, interrupt handling delay, and system loads. These factors, if not controlled, can easily add up to several milliseconds on average, which translates to several feet of ranging error.

We show the general system model of BeepBeep design [34] in Fig. 2.5, in which each device is equipped with a speaker and a microphone, denoted by  $S_A, M_A$  in device  $A$  and  $S_B, M_B$  in device  $B$ , respectively. BeepBeep ranging scheme takes three steps:

1. *Two-way sensing.* As shown in Fig. 2.5, both devices are initially in recording state. Device  $A$  first emits a sound signal through its speaker  $S_A$ . This signal will be recorded by its own microphone as well as the other device  $B$ . Then, after an arbitrary delay, device  $B$  emits another sound signal back through its speaker  $S_B$ . This signal is also recorded by both microphones on the two devices.
2. *EToA computation.* Both devices examine their recorded data and locate the sample points when the two previously emitted signals arrive. The time

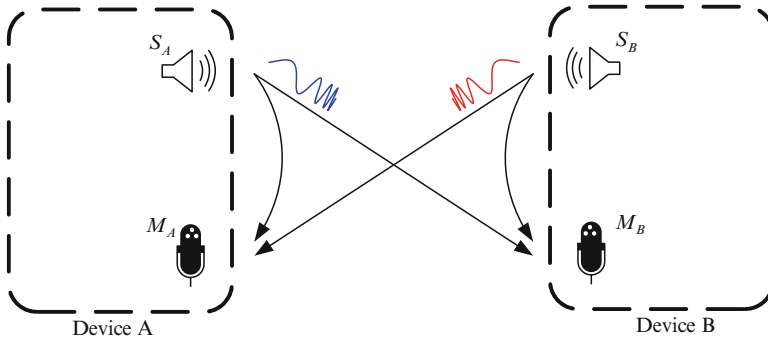


**Fig. 2.5** The system model of the BeepBeep design

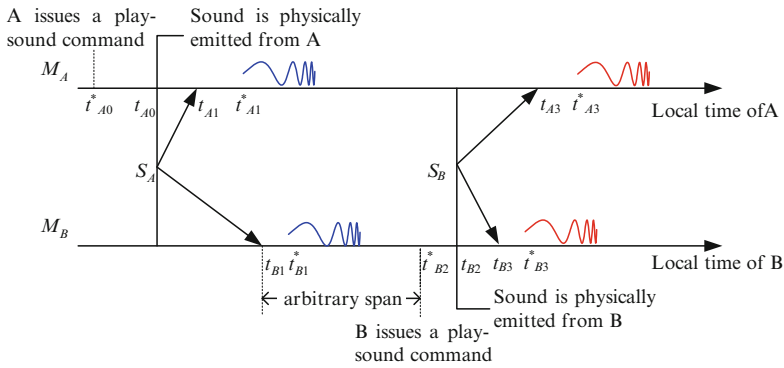


**Fig. 2.6** Illustration of event sequences in BeepBeep ranging procedure

difference between these two signals is denoted as elapsed time between the two time of arrivals (EToA). When the EToA is computed, the two devices will exchange their locally measured EToA.

3. *Distance estimation.* The distance between the two devices is computed based on these two values of EToA.

Figure 2.6 shows the signal transmission procedure and timing relation among events in the first stage. Two time lines are drawn in the figure with the upper one representing the local time of device A and the bottom one the local time of device B. Let  $t_{A0}^*$  denote the time when device A instructs its speaker to emit the sound signal. Due to the sending uncertainty, however, the actual time when the speaker physically emits might be  $t_{A0}$ . The time the signal arrives at the microphones of devices A and B is marked  $t_{A1}$  and  $t_{B1}$ , respectively. Again, due to the receiving uncertainty, applications on device A and B may obtain these signal data only at time  $t_{A1}^*$  and  $t_{B1}^*$ . Similarly, let  $t_{B2}^*$  and  $t_{B2}$  denote the time when device B instructs to send out a sound signal and when the signal is physically out;  $t_{A3}$  and  $t_{B3}$

denote the time when the signal from device  $B$  arrives at the microphones of device  $A$  and  $B$ ; and  $t_{A3}^*$  and  $t_{B3}^*$  denote the time when the applications on device  $A$  and  $B$  conclude the arrival of the signal data.

Let  $d_{x,y}$  denote the distance between the device  $x$ 's speaker to device  $y$ 's microphone. From Fig. 2.6, we have

$$\begin{aligned} d_{A,A} &= c(t_{A1} - t_{A0}), \\ d_{A,B} &= c(t_{B1} - t_{A0}), \\ d_{B,A} &= c(t_{A3} - t_{B2}), \\ d_{B,B} &= c(t_{B3} - t_{B2}), \end{aligned}$$

where  $c$  is the speed of sound. Then, the distance  $D$  between the two devices can be approximated as

$$\begin{aligned} D &= \frac{1}{2}(d_{A,B} + d_{B,A}) \\ &= \frac{c}{2}((t_{B1} - t_{A0}) + (t_{A3} - t_{B2})) \\ &= \frac{c}{2}((t_{A3} - t_{A1}) - (t_{B3} - t_{B1}) + (t_{B3} - t_{B2}) + (t_{A1} - t_{A0})) \\ &= \frac{c}{2}((t_{A3} - t_{A1}) - (t_{B3} - t_{B1}) + d_{B,B} + d_{A,A}). \end{aligned}$$

In this equation, the latter two terms are the distances between the speaker and the microphone of the two devices. This distance is a constant to a certain device and can be measured a priori. Therefore, the distance between two devices is determined solely by the first two terms, which are actually the EToA values measured on device  $A$  and  $B$ , respectively. Note that EToA is calculated by each individual device independently, i.e., without referring any timing information on the other device, so that no clock synchronization between devices is needed. Moreover, due to the self-recording strategy, all time measurements are associated with the arrival instants of the sound signals, and, therefore, the sending uncertainty is also removed.

Obtaining the exact time instance when the signal arrives is difficult due to the indeterministic latency introduced by hardware and software (receiving uncertainty). Hence, the values of  $t_{A0}$ ,  $t_{A1}$ ,  $t_{A3}$ ,  $t_{B1}$ ,  $t_{B2}$ , and  $t_{B3}$  cannot be accurately measured. BeepBeep solves this issue by not referring to any local clock while inferring timing information directly from recorded sound samples.

As the received sound signal is always sampled at a fixed frequency (represented by  $f_s$ ) by the A/D converter, BeepBeep directly obtains EToA by counting the sample number between the two ToAs of signals from recorded data, without dealing with the local clock of the end system. Thus, the accuracy depends on the fidelity of the recording module. Since all the sound signals are recorded, BeepBeep



only needs to check the recorded data and identify the first sample point of each signal. Then, EToA is obtained by counting the number of samples between the two sound signals.

With sample counting, the above equation can be rewritten as

$$D = \frac{c}{2} \left( \frac{n_{A3} - n_{A1}}{f_{sA}} - \frac{n_{B3} - n_{B1}}{f_{sB}} \right) + K,$$

where  $n_x$  denotes the index of the sample point at instant  $t_x$ ,  $f_{sA}$  and  $f_{sB}$  are the sampling frequency of device  $A$  and  $B$ , respectively, and  $K = d_{B,B} + d_{A,A}$  is a constant. Assume the sampling frequency to be 44.1 kHz, since the 44.1 kHz sampling frequency is the basic, de facto standard that almost every sound card supports. In this case, we have  $f_{sA} = f_{sB}$ , and the above equation can be simplified to

$$D = \frac{c}{2f_s} ((n_{A3} - n_{A1}) - (n_{B3} - n_{B1})) + K.$$

From this equation, the measurement granularity is positively proportional to the sound speed  $c$  and inversely proportional to the sampling frequency  $f_s$ . Take a typical setting of  $c = 340$  m/s and  $f_s = 44.1$  kHz, the distance granularity is then about 0.77 cm.

The distance granularity shows the best accuracy for BeepBeep system. In practice, due to several constraints, such as the signal to noise ratio, the multipath effects, and signal distortion, BeepBeep can achieve 1 or 2 cm accuracy. Experiments show that the operational range for the indoor cases is around 4 m and that for outdoor cases is in general larger than 10 m.

Being accurate, ToA systems are generally constrained by the line-of-sight condition, which is often difficult to meet in some environments. In addition, ToA systems perform better when they are calibrated properly, since speakers and microphones never have identical transmission and reception characteristics. Furthermore, the speed of sound in air varies with air temperature and humidity, which introduce inaccuracy into distance estimation. Acoustic signals also show multipath propagation effects that may impact the accuracy of signal detection. These can be mitigated to a large extent using simple spread-spectrum techniques [35]. The basic idea is to send a pseudorandom noise sequence as the acoustic signal and use a matched filter for detection, instead of using a simple chirp and threshold detection.

By designing BeepBeep, a high-accuracy acoustic-based ranging system, the localization can achieve 1 or 2 cm accuracy within a range of more than 10 m, which is so far the best result of ranging with off-the-shelf devices. Many localization algorithms use ToA simply because it is dramatically more accurate than radio-only methods. The trade-off is that nodes must be equipped with acoustic transceivers in addition to radio transceivers.

### 2.1.3 Time Difference of Arrival (TDoA)

When multiple reference nodes are available, there is a category of measurements called TDoA. The transmitter sends a signal to a number of receivers at known locations. Then, the receivers record the arrival time of the signal, as illustrated in Fig. 2.7. The location of the transmitter is computed by the difference of the recorded arrival timestamps. The TDoA between a pair of receivers  $i$  and  $j$  is given by

$$\Delta t_{ij} \triangleq (t_i - t_0) - (t_j - t_0) = t_i - t_j = \frac{1}{c} (\|r_i - r_t\| - \|r_j - r_t\|) \quad i \neq j$$

where  $t_0$  is the time when the signal is sent from the transmitter (located at  $r_t$ ),  $t_i$  and  $t_j$  are the times when the signal is received at receivers  $i$  (located at  $r_i$ ) and  $j$  (located at  $r_j$ ), respectively,  $c$  is the speed of the signal, and  $\|\cdot\|$  denotes the Euclidean norm. TDoA is also known as range difference since the speed of signal is assumed to be known a priori.

Accurate TDoA measurement relies on two issues, time synchronization of receivers and signal detection, both of which are well known and still challenging. In the TDoA scheme, receivers need to be precisely synchronized to make the time difference  $(t_i - t_j)$  valid. Even tiny errors of synchronization can totally destroy the final location results since the commonly used wireless signals travel fast (e.g., about 343 m/s for acoustic signals) or ultimately fast (e.g.,  $3 \times 10^8$  m/s for radio signals).

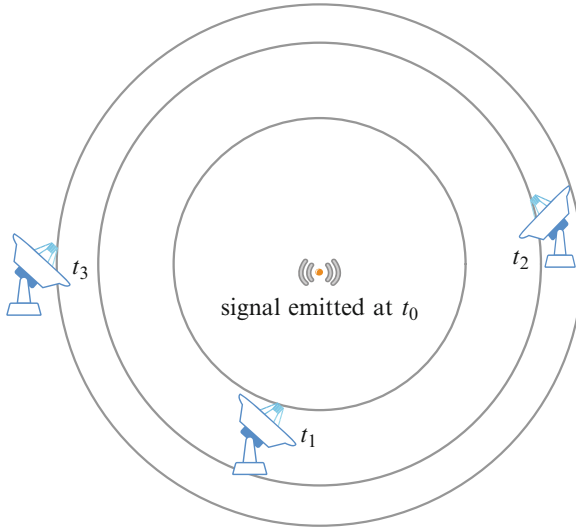


Fig. 2.7 TDOA measurement

Measuring the TDoA of a signal at two receivers at separate locations is a relatively mature field. The most widely used method is the generalized cross-correlation method [36], where the cross-correlation function between two signals  $s_i$  and  $s_j$  received at receivers  $i$  and  $j$  is given by integrating the lag product of two received signals for a sufficiently long time period  $T$ :

$$\rho_{i,j}(\tau) = \frac{1}{T} \int_0^T s_i(t) s_j(t - \tau) dt.$$

TDoA only requires the receivers to be synchronized and does not demand any synchronization between the transmitter and the receivers. However, intensive computation is introduced and performed at receivers. Hence, it especially suits for the networks with powerful infrastructures, such as the cellular network.

## 2.2 Angle Measurement

Another possibility for localization is the use of angular estimates instead of distance estimates. In trigonometry and geometry, triangulation is the process of determining the location of a point by measuring angles to it from two known reference points (as illustrated in Fig. 2.8), using the law of sines. Triangulation is once used to find the coordinates and sometimes the distance from a ship to the shore.

The angle of arrival (AoA), a.k.a., direction of arrival (DOA), measurement is typically gathered using radio or microphone arrays, which allow a receiver to determine the direction of a transmitter. Suppose, several (3–4) spatially separated microphones hear a single transmitted signal. By analyzing the phase or time difference between the signal's arrival's at different microphones, it is possible to discover the AoA of the signal.

These methods can obtain accuracy within a few degrees [37]. A very simple localization technique, involving three rotating reference beacons at the boundary of a sensor network providing localization for all interior nodes, is described in [38].

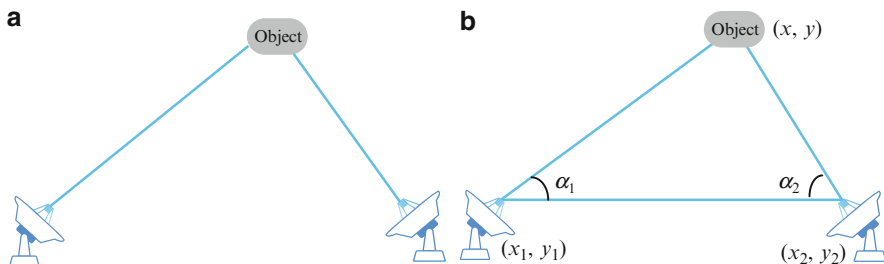


**Fig. 2.8** Angle measurement

Unfortunately, AoA hardware tends to be bulkier and more expensive than ToA or TDoA ranging hardware, since each node must have one speaker and several microphones. Furthermore, the need of spatial separation between microphones is difficult to be accommodated in small size devices.

## 2.3 Area Measurement

If the radio or other signal coverage region can be described by a geometric shape, this can be used to provide location estimates by determining which geometric areas that a node is in. The basic idea of area estimation is to compute the intersection of all overlapping coverage regions and choose the centroid as the location estimate. Along with the increasing number of constraining areas, higher localization accuracy can be achieved.

According to how the area is estimated, we classify the existing ideas into two categories: single reference area estimation and multireference area estimation.

### 2.3.1 Single Reference Area Estimation

Single reference estimation means that areas are obtained in a pairwise manner, i.e., the information of a geometric area comes from only one reference at each stage. For instance, the region of radio coverage may be upper bounded by a circle of radius  $R_{\max}$ . In other words, if node  $B$  hears node  $A$ , it knows that it must be no more than a distance  $R_{\max}$  from  $A$ . If an unknown node hears from several reference nodes, it can determine that it must lie in the geometric region described by the intersection of circles of radius  $R_{\max}$  centered at reference nodes, as illustrated in Fig. 2.9a. This can be extended to other scenarios. For instance when both the lower bound  $R_{\min}$  and the upper bound  $R_{\max}$  can be determined, based on the received signal strength, the shape of a single node's coverage is an annulus, as illustrated in Fig. 2.9c; when an angular sector ( $\theta_{\min}, \theta_{\max}$ ) and a maximum range  $R_{\max}$  can be determined, the shape for a single node's coverage would be a cone with given angle and radius, as illustrated in Fig. 2.9d.

Localization using geometric regions is first described in [39]. One of the nice features of these techniques is that not only the unknown nodes can use the centroid of the overlapping region as a specific location estimate if necessary, but also they can determine a bound on the location error using the size of this region. When the upper bounds on these regions are tight, the accuracy of this geometric approach can be further enhanced by incorporating “negative information” about which reference nodes are not within the range [40]. Although arbitrary shapes can be potentially computed in this manner, a computational simplification to determine this bounded region is to use rectangular bounding boxes. Reference nodes by some way define several bounding boxes; an unknown node estimates its location according to the intersection of all boxes, which can be efficiently computed.

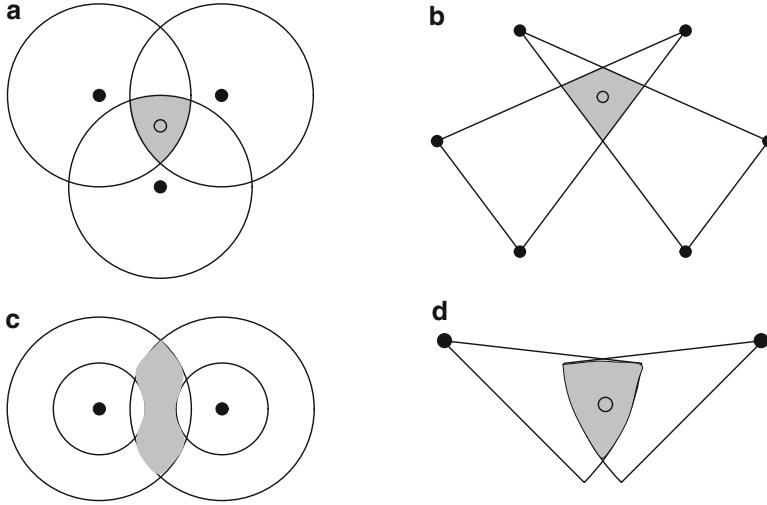


Fig. 2.9 Area measurements

### 2.3.2 Multireference Area Estimation

Another approach of area estimation is the approximate point in triangle (APIT) technique [41]. Its novelty lies in that regions are defined as triangles between different sets of three reference nodes, rather than the coverage of a single node.

APIT consists of two key processes: triangle intersection and point in triangle (PIT) test. Nodes are assumed to hear a fairly large number of beacons. A node forms some number of “reference triangles”: the triangle formed by three arbitrary references. The node then decides whether it is inside or outside a given triangle by PIT test. Once the process is complete, the node finds the intersection of the reference triangles that contain it and chooses the centroid as its position estimate, as illustrated in Fig. 2.9b. During process, APIT does not assume that nodes can range to these beacons.

The PIT test is based on geometry. For a given triangle with points  $A$ ,  $B$ , and  $C$ , a point  $M$  is outside triangle  $ABC$ , if there exists a direction such that a point adjacent to  $M$  is further/closer to points  $A$ ,  $B$ , and  $C$  simultaneously. Otherwise,  $M$  is inside triangle  $ABC$ . Unfortunately, given that typically nodes cannot move, an approximate PIT test is proposed based on two assumptions. The first one is that the range measurements are monotonic and calibrated to be comparable but are not required to produce distance estimates. The second one assumes sufficient node density for approximating node movement. If no neighbor of  $M$  is further from/closer to all three anchors  $A$ ,  $B$ , and  $C$  simultaneously,  $M$  assumes that it is inside triangle  $ABC$ . Otherwise,  $M$  assumes it resides outside this triangle. In practice, however, this approximation does not realize the PIT test well. Nevertheless, APIT provides a novel point of view to do localization based on area estimation.

## 2.4 Hop Count Measurements

Based on the observation that if two nodes can communicate by radio, their distance from each other is less than  $R$  (the maximum range of their radios) with high probability, many delicate approaches are designed for accurate localization. In particular, researchers have found “hop count” to be a useful way to compute internode distances. The local connectivity information provided by the radio defines an unweighted graph, where the vertices are wireless nodes and edges represent direct radio links between nodes. The hop count  $h_{ij}$  between nodes  $s_i$  and  $s_j$  is then defined as the length of the shortest path from  $s_i$  to  $s_j$ . Obviously, the physical distance between  $s_i$  and  $s_j$ , namely,  $d_{ij}$ , is less than  $R \times h_{ij}$ , the value which can be used as an estimate of  $d_{ij}$  if nodes are densely deployed.

Another method to estimate per-hop distance is to employ a number of anchor nodes, as illustrated in Fig. 2.10. As the locations of anchor nodes are known, the distance between them can be readily computed. Hence, if the hop count  $h_{ij}$  between two references ( $s_i$  and  $s_j$ ) and the distance  $d_{ij}$  are available, the per-hop distance can be estimated as  $d_{\text{hop}} = d_{ij}/h_{ij}$ .

Due to the hardware limitations and energy constraints of wireless devices, hop-count-based localization approaches are cost-effective alternatives to range-based approaches. Since there is no way to measure physical distances between nodes, existing hop-count-based approaches largely depend on connectivity measurements with a high density of anchors.

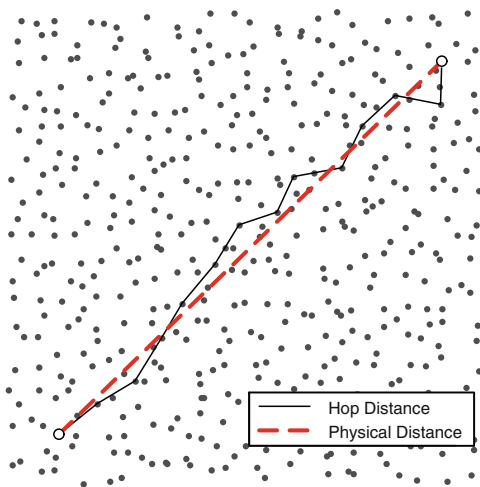
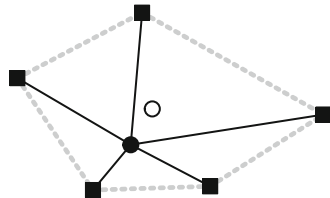


**Fig. 2.10** Hop count measurement

**Fig. 2.11**  $k$ -neighbor proximity



## 2.5 Neighborhood Measurement

Radio connectivity can be considered economic since no extra hardware is required. Perhaps the most basic location technique is that of one-neighbor proximity, involving a simple decision of whether two nodes are within reception range of each other. A set of reference nodes is placed in the network with some nonoverlapping (or nearly nonoverlapping) subregions. Reference nodes periodically emit beacons including their location IDs. An unknown node uses the received location information as its own location, achieving a course-grained localization. The major advantage of this single-neighbor proximity approach is the simplicity of computation.

The neighborhood information can be more useful when the density of reference nodes is sufficiently high that there are several reference nodes within the range of an unknown node. Let there be  $k$  reference nodes within the proximity of the unknown node, as illustrated in Fig. 2.11. Suppose black squares are references and the black circle is the real location of the unknown node. We use the centroid (denoted by the hollow circle) of the polygon constructed by the  $k$  reference nodes as the estimated position of the unknown node. This is actually a  $k$ -nearest-neighbor approximation in which all reference nodes have equal weights.

This simple centroid technique has been investigated using a model with each node having a simple circular range  $R$  in an infinite square mesh of reference nodes spaced a distance  $d$  apart [42]. It is shown through simulation that, as the overlap ratio  $R/d$  is increased from 1 to 4, the average error in localization decreases from  $0.5d$  to  $0.25d$ .

The  $k$ -neighbor proximity approach inherits the merit of computational simplicity from the single-neighbor proximity approach; while at the same time, it provides more accurate localization results than the single-neighbor proximity statistically.

## 2.6 Summary

In this section, a comparative study is presented for the existing physical measurement approaches. Table 2.1 provides an overview of these approaches in terms of accuracy, hardware cost, and environment requirements. All approaches have their own merits and drawbacks, making them suitable for different applications.

**Table 2.1** Comparative study of physical measurements

Physical Measurements		Accuracy	Hardware cost	Computation cost
Distance	RSS	Median	Low	Low
	ToA	High	High	Low
Angle	AoA	High	High	Low
Area	Single reference	Median <sup>a</sup>	Median <sup>a</sup>	Median
	Multireference	Median <sup>a</sup>	Median <sup>a</sup>	High
Hop count	Per-hop distance	Median	Low	Median
Neighborhood	Single neighbor	Low	Low	Low
	Multineighbor	Low	Low	Low

<sup>a</sup>Depends on the diverse geometric constrains

Recent technical advances foster a novel ranging approaches. Ultra-wideband (UWB) is a radio technology that can be used at very low energy levels for short-range high-bandwidth communications by using a large portion of the radio spectrum [43]. It has relative bandwidth larger than 20% or absolute bandwidth of more than 500 MHz. Such wide bandwidth offers a wealth of advantages for both communications and ranging applications. In particular, a large absolute bandwidth offers high resolution with improved ranging accuracy of centimeter level.

UWB has a combination of attractive properties for in-building location systems. First, it is a non-line-of-sight technology with a range of a few tens of meters, which makes it practical to cover large indoor areas; second, it is easy to filter the signal to minimize the multipath distortions that are the main cause of inaccuracy in RF-based location systems. With conventional RF, reflections in in-building environments distort the direct path signal, making accurate pulse timing difficult; while with UWB, the direct path signal can be distinguished from the reflections. These properties provide a good cost-to-performance ratio of all available indoor location technologies.

In some positioning systems, two or more types of physical measurements, studied in previous subsections, are used simultaneously in order to obtain more information about the target node and increase the accuracy and robustness of positioning. Examples of such multimodal (or hybrid) scheme include ToA/AoA [44], ToA/RSS [45], TDoA/AoA [46], and ToA/TDoA [47]. Recently, some progresses from computational geometry reveal the great potential of multimodal measurements, regarding localization accuracy. With the rapid development of integrated circuits, multimodal measurement has been available on many wireless devices, especially sensor nodes.

In all ranging algorithms discussed above, nodes should actively participate in the ranging process, i.e., sending or receiving radio signals, or measuring physical data. For some applications, however, the to-be-located objects cannot join the process, and it is also difficult to attach networked nodes to them. One typical application is intrusion detection, in which it is impossible and unreasonable to equip intruders with locating devices. To tackle this issue, recently a novel concept of device-free localization, also called transceiver-free localization, is proposed [48, 49].



Device-free localization is envisioned to be able to detect, localize, track, and identify entities free of devices and works by processing the environment changes collected at scattering monitoring points. Existing work focuses on analyzing RSS changes, and often suffers from high false positives. How to design a device-free localization system which can provide accurate locations is a challenging and promising research problem.



<http://www.springer.com/978-1-4419-7370-2>

Location, Localization, and Localizability

Location-awareness Technology for Wireless Networks

Liu, Y.; Yang, Z.

2011, XIII, 154 p., Hardcover

ISBN: 978-1-4419-7370-2